Journal of Statistical Physics, Vol. 38, Nos. 5/6, 1985

Two-Body Correlations and Pair Formation in the Two-Dimensional Coulomb Gas

J. P. Hansen[1,2] and P. Viot[1]

Received June 14, 1984; revised October 4, 1984

We investigate pair correlations in the two-dimensional Coulomb gas made up of two species of point ions carrying electric charges $Z_1 e(>0)$ and $Z_2 e(<0)$, and interaction by the logarithmic Coulomb potential. This system is known to be classically stable for couplings $\Gamma = e^2/k_B T < T_c = 2/|Z_1 Z_2|$ (where T is the temperature). Correlations between equally charged ions are shown to be greatly modified at short distances, in the range $\Gamma_c/2 < \Gamma < \Gamma_c$, due to gradual ion "condensation." The usual integral equations for the pair correlation functions admit no solutions in that range. Preliminary Monte Carlo simulations for the symmetric case ($Z_1 = -Z_2$) reveal a striking "chemical" equilibrium between tightly bound ion pairs and free ions, which is reasonably well described by a simple Bjerrum model.

KEY WORDS: Two-dimensional Coulomb gas; pair correlation functions; integral equations; ion pairing; Monte Carlo simulations.

1. INTRODUCTION

Two-dimensional Coulomb systems of charged particles interacting through a logarithmic potential have recently attracted much attention for a number of reasons. The one-component version of equally charged point ions in a uniform neutralizing background is exactly soluble for one particular (nontrivial) value of the coupling $\Gamma = e^2/k_B T$, namely $\Gamma = 2$.[1] Systems of oppositely charged hard-core ions undergo a transition from a high-temperature Coulomb gas phase to a low-temperature dipolar gas phase at some density-dependent temperature; this is the so-called

[1] Laboratoire de Physique Théorique des Liquides, Equipe associée au CNRS, Université Pierre et Marie Curie, 75230 Paris Cedex 05, France.
[2] École Normale Supérieure de Saint-Cloud, 92211 Saint-Cloud, France.

0022-4715/85/0300-0823$04.50/0

Kosterlitz–Thouless transition,[2] which is the prototype of a class of phase transitions without spontaneous symmetry breaking; the decay of correlations changes only from exponential in the high-temperature phase to a power law in the low-temperature phase.[3] The lattice version of the two-component Coulomb gas has been shown to be isomorphous, through a duality transformation, to the discrete Gaussian model for the roughening transition.[4]

In this paper we return to the continuous Coulomb gas of oppositely charged *point* ions (no hard core) for which a number of important results are already available. Whereas the stability of three-dimensional Coulomb matter requires quantum mechanics (in particular Fermi statistics),[5] the purely classical two-dimensional Coulomb gas is stable against collapse of oppositely charged ions pairs above the critical temperature $T_c = e^2/(2k_B)$.[6,7] Moreover, the existence of the thermodynamic limit, and the absence of a phase transition for this model above T_c, can be proved rigorously.[7,8] In this work we focus on pair correlation functions, which have not been investigated quantitavely so far for this model. In addition, while the published literature deals exclusively with the symmetric Coulomb gas involving equal numbers of ions carrying opposite charges $\pm e$, we consider explicitly the more general, asymmetric case of ions of different absolute valences.

Our interest in the two-dimensional Coulomb gas stems from previous work on the strongly coupled electron–proton plasma in three dimensions, above the degeneracy temperature of the electrons.[9] This plasma is classically unstable against electron–proton collapse at any temperature, and in a semiclassical treatment the infinite Coulomb attraction between oppositely charged particles is tempered for distances shorter than the de Broglie thermal wavelength via the use of effective pair potentials which account approximately for quantum diffraction and symmetry effects.[10] The corresponding Hamiltonian is then temperature dependent, and this circumstance introduces some ambiguities which are avoided in the corresponding two-dimensional model above the critical temperature T_c where the pure (logarithmic) Coulomb potential can be used. The two-dimensional Coulomb gas allows the physics of ion–electron recombination near T_c to be studied in purely classical terms. Hence we consider the two-dimensional Coulomb gas to be a useful model for an investigation of strongly coupled, nondegenerate ion–electron plasma, and in particular of strongly magnetized plasmas[8] where guiding centers can be looked upon, in a first approximation, as infinitely long parallel wires. It is interesting to note that the value of the Coulomb coupling constant at the two-dimensional collapse temperature, $\Gamma_c = e^2/k_B T_c = 2$, is typical of the couplings achieved in inertial confinement fusion experiments. It is also

worth mentioning that much of the simulation work on such dense fusion plasmas is carried out with two-dimensional codes.

The paper is organized as follows. Definitions, sum rules, and general properties of pair correlation functions and their relations to thermodynamics are summarized in Section 2. In Section 3 we focus on the behavior of pair correlations at short distances and we show in particular that correlations between equal charge ions are weakened near the collapse temperature due to pair formation. In Section 4 we present some quantitative results for the pair correlation functions obtained from approximate theories, and we show the limitations of the standard integral equations. Section 5 is devoted to a Monte Carlo study of pair formation near the collapse temperature, while concluding remarks are made in Section 6. A preliminary account of some of the results of Section 4 has been published elsewhere.[11]

2. PAIR CORRELATIONS AND THERMODYNAMICS

The asymmetric two-dimensional Coulomb gas is made up of two species of particles carrying electric charges $Z_\alpha e$ ($\alpha = 1, 2$), where e is some elementary charge. If $n_\alpha = N_\alpha/S$ denotes the number of particles of species α per unit area, overall charge neutrality requires that

$$Z_1 n_1 + Z_2 n_2 = 0 \tag{1}$$

If the model is to represent an ion–electron plasma, $Z_1 > 0$ will be the (integer) valence of the ions or nuclei while $Z_2 = -1$ for the electrons. In this case the ratio $z = |Z_1/Z_2|$ is an integer, and in particular for the symmetric Coulomb gas, $z = 1$ (e.g., protons and electrons). The total number density of the system will be denoted by $n = N/S = n_1 + n_2$, and a convenient length scale will be the "ion-disk radius":

$$a_1 = (\pi n_1)^{-1/2} \tag{2}$$

The bare Coulomb potential due to a charge of species α located at the origin is, in two dimensions,

$$\psi_\alpha^{(0)}(r) = -Z_\alpha e \ln(r/L) \tag{3}$$

where L is an arbitrary scale factor which fixes the zero of energy. The corresponding potential energy of a pair will be denoted by

$$v_{\alpha\beta}(r) = Z_\beta e \psi_\alpha^{(0)}(r) = Z_\alpha e \psi_\beta^{(0)}(r) \tag{4}$$

The canonical partition function of the system reads:

$$\mathcal{Q}_N = \frac{Q_N}{N_1!\, N_2!\, \lambda_1^{N_1} \lambda_2^{N_2}} \tag{5}$$

where λ_α is the de Broglie thermal wavelength of spcies α, and Q_N is the classical configuration integral:

$$\begin{aligned} Q_N &= \int_S \cdots \int_S \exp\left\{ \frac{e^2}{k_B T} \sum\sum_{i<j} Z_i Z_j \ln(r_{ij}/L) \right\} \prod_{i=1}^{N} d^2 r_i \\ &= \int_S \cdots \int_S \prod_{i<j} (r_{ij}/L)^{\Gamma Z_i Z_j} \prod_i d^2 r_i \\ &= S^{N(1+\Gamma Z_1 Z_2/4)}\, L^{-\Gamma N Z_1 Z_2/2}\, Q_N^*(\Gamma) \end{aligned} \tag{6}$$

The reduced configuration integral

$$Q_N^*(\Gamma) = \int_1 \cdots \int_1 \prod_{i<j} s_{ij}^{\Gamma Z_i Z_j} \prod_{i=1}^{N} d^2 s_i \tag{7}$$

depends only on the dimensionless Coulomb coupling constant

$$\Gamma = \frac{e^2}{k_B T} \tag{8}$$

and not on the density; in Eq. (7) the dimensionless integration variables are $\mathbf{s}_i = \mathbf{r}_i / S^{1/2}$. The configuration integral is finite as long as

$$\Gamma < \Gamma_c = \frac{2}{|Z_1 Z_2|} \tag{9}$$

i.e., as long as the temperature is above the critical (collapse) value:

$$T_c = \frac{e^2}{2k_B |Z_1 Z_2|} \tag{10}$$

Since the dependence on the surface S factors out explicitly in Eq. (6), the equation-of-state for $\Gamma < \Gamma_c$ is trivially given by[12,6]

$$\frac{PS}{Nk_B T} = 1 + \frac{1}{4} Z_1 Z_2 \Gamma \tag{11}$$

The exact result (11) simply reflects the fact that the density is an irrelevant variable for the two-dimensional Coulomb gas. The nontrivial part of the

reduced thermodynamic quantities depends only on the single variable Γ. Whereas the density derivatives of the excess free energy $F = -k_B T \ln Q_N$ can all be calculated exactly, like the pressure, the temperature derivatives, like the internal energy U or the constant surface specific heat c_s, are non-trivial quantities, which can only be calculated within some approximation scheme, or by computer "experiments." Note that the constant pressure specific heat c_p is related to c_s by

$$\frac{c_p - c_s}{N k_B} = \frac{1}{1 + \frac{1}{4} Z_1 Z_2 \Gamma} \tag{12}$$

The microscopic structure of the Coulomb gas is characterized in the usual fashion by three partial pair distribution functions $g_{\alpha\beta}(r)$, or equivalently by their Fourier transforms, the partial structure factors

$$\begin{aligned} S_{\alpha\beta}(k) &= \frac{1}{N} \langle \rho_{\mathbf{k}\alpha} \rho^*_{\mathbf{k}\beta} \rangle \\ &= x_\alpha \delta_{\alpha\beta} + x_\alpha x_\beta \hat{h}_{\alpha\beta}(k) \end{aligned} \tag{13}$$

where

$$\begin{aligned} \hat{h}_{\alpha\beta}(k) &= n \int e^{i\mathbf{k}\cdot\mathbf{r}} h_{\alpha\beta}(r)\, d^2 r \\ &= 2\pi n \int_0^\infty h_{\alpha\beta}(r)\, J_0(kr) r\, dr \end{aligned} \tag{14}$$

$$h_{\alpha\beta}(r) = g_{\alpha\beta}(r) - 1 \tag{15}$$

and the x_α are the concentrations $x_\alpha = n_\alpha / n$.

The direct correlation functions $c_{\alpha\beta}(r)$ form an alternative set which is very useful in constructing approximate theories of the pair structure; they are defined via the usual Ornstein–Zernike (OZ) relations, which read in Fourier space:

$$\hat{h}_{\alpha\beta}(k) = \hat{c}_{\alpha\beta}(k) + \sum_\gamma \hat{c}_{\alpha\gamma}(k)\, x_\gamma \hat{h}_{\gamma\beta}(k) \tag{16}$$

The pair distribution functions obey the Stillinger–Lovett sum rules[13]:

$$2\pi n \sum_\gamma x_\gamma Z_\gamma \int_0^\infty h_{\alpha\gamma}(r) r\, dr = -Z_\alpha, \qquad \alpha = 1, 2 \tag{17a}$$

$$2\pi n \sum_\alpha \sum_\gamma x_\alpha x_\gamma Z_\alpha Z_\gamma \int_0^\infty h_{\alpha\gamma}(r) r^3\, dr = \frac{4 Z_1 Z_2}{k_D^2} \tag{17b}$$

where k_D is the inverse Debye length:

$$k_D^2 = \frac{2\pi e^2}{k_B T}[n_1 Z_1^2 + n_2 Z_2^2]$$
$$= -2\pi n \Gamma Z_1 Z_2 \tag{18}$$

Equation (17a) is merely an expression of local charge neutrality around an ion of species α. Equation (17b) can be proven in a number of ways. In the original derivation[13] the result follows from the perfect screening condition stating that the inverse static dielectric function $1/\varepsilon(k)$ must vanish for a conductor in the $k \to 0$ limit. The perfect screening condition (17b) follows also from a simple assumption concerning the direct correlation function $c_{\alpha\beta}(r)$.[14] If the latter are separated into their asymptotic part, $-v_{\alpha\beta}(r)/k_B T$, and their short-range part, $c^s_{\alpha\beta}(r)$, i.e., in Fourier space

$$\hat{c}_{\alpha\beta}(k) = \frac{Z_\alpha Z_\beta}{Z_1 Z_2}\frac{k_D^2}{k^2} + \hat{c}^s_{\alpha\beta}(k) \tag{19}$$

the assumption is that $\hat{c}^s_{\alpha\beta}(k)$ is a regular function in the $k \to 0$ limit. This, combined with the OZ relations (16), leads directly back to Eqs. (17). Very recently the perfect screening sum rule (17b) has been proven rigorously on the basis of the Born–Green–Yvon hierarchy and a clustering assumption.[15] More generally these clustering assumptions imply a whole set of sum roles involving two-body and higher-order distribution functions which must be obeyed by any Coulomb system, and in particular by the two-dimensional Coulomb gas.[16]

A number of thermodynamic properties are expressible in terms of the pair functions. The virial theorem in conjunction with the local neutrality condition (17a) leads immediately back to the equation of state (11). The excess internal energy can be calculated from the standard relation

$$u = \frac{U^{\text{ex}}}{Ne^2} = \sum_\alpha \sum_\beta x_\alpha x_\beta \frac{n}{2e^2} \int g_{\alpha\beta}(r)\, v_{\alpha\beta}(r)\, d^2 r$$
$$= -\sum_\alpha \sum_\beta x_\alpha x_\beta Z_\alpha Z_\beta \pi n \int_0^\infty h_{\alpha\beta}(r) \ln(r/L) r\, dr$$
$$= -x_1 Z_1^2 \int_0^\infty [h_{11}(x) - 2h_{12}(x) + h_{22}(x)] \ln(x) x\, dx$$
$$+ \frac{Z_1 Z_2}{2} \ln\left(\frac{L}{a_1}\right) \tag{20}$$

where we made repeated use of the global and local charge neutrality conditions (1) and (17a); x denotes the reduced distance r/a_1. Since the interactions are purely Coulombic, the excess internal energy can also be expressed in terms of the mean electric potential acting on the ions of each species. The local excess charge density around an ion of species α, $\rho_\alpha(\mathbf{r})$, is related to the electric potential $\psi_\alpha(\mathbf{r})$ by Poisson's equation:

$$\nabla^2\psi_\alpha(\mathbf{r}) = -2\pi e\rho_\alpha(\mathbf{r})$$

$$= -2\pi ne\sum_\gamma x_\gamma Z_\gamma h_{\alpha\gamma}(r) \tag{21}$$

$\psi_\alpha(\mathbf{r})$ is the sum of the bare Coulomb potential $\psi_\alpha^{(0)}(r)$ of the ion at the origin and of the potential due to the local charge distribution around that ion:

$$\psi_\alpha(\mathbf{r}) = \psi_\alpha^{(0)}(\mathbf{r}) + \psi_\alpha^*(\mathbf{r}) \tag{22}$$

Equation (23) for u is now rewritten as

$$u = -\frac{1}{2}\sum_\alpha x_\alpha Z_\alpha \int \rho_\alpha(\mathbf{r}) \ln(r/L)\, d^2r$$

$$= \frac{1}{2e}\left[x_1 Z_1 \psi_1^*(0) + x_2 Z_2 \psi_2^*(0)\right] + \frac{Z_1 Z_2}{2}\ln\left(\frac{L}{a_1}\right) \tag{23}$$

after use of Eq. (21) and integration by parts.

The isothermal compressibility $\chi_T = (\partial n/\partial P)_T/n$ is related to the $k \to 0$ limit of the partial structure factors[17]:

$$\lim_{k\to 0}(x_\alpha x_\beta)^{-1} S_{\alpha\beta}(k) = nk_B T\chi_T = \frac{1}{1+\frac{1}{4}\Gamma Z_1 Z_2} \tag{24}$$

where use was made of the exact equation-of-state (11). The relations listed above will be used to calculate thermodynamic properties of the two-component plasma within various approximation schemes (Section 4) and from Monte Carlo simulations (Section 5). The symmetric version of the model ($Z_1 = -Z_2 = 1$) is invariant under charge conjugation; the pair structure is then entirely characterized by two correlation functions only, $g_{11}(r) = g_{22}(r)$ and $g_{12}(r)$. The symmetric model undergoes a single recombination, at $\Gamma = 2$; beyond this value of the coupling constant the pressure of the system behaves as that of an ideal gas of $N/2$ neutral particles composed of two oppositely charged ions which have recombined.[6] The asymmetric case is more interesting since it leads to several successive recombinations, reminiscent of counterion "condensation" in polyelectrolytes.[18] Consider

the case where $z = |Z_1/Z_2|$ is integer and choose $Z_2 = -1$ so that $z = Z_1$; at each recombination the valence of the positive ions is reduced by one and the total number of negative ions or electrons drops by N_1. The equation-of-state is a succession of straight line segments:

$$\frac{\beta P}{n} = 1 - \frac{\Gamma z}{4}, \qquad 0 < \Gamma < \frac{2}{z}$$

$$\frac{\beta P}{n} = \frac{z+1-\zeta}{z+1}\left[1 - \frac{\Gamma}{4}(z-\zeta)\right]$$

$$\frac{2}{z+1-\zeta} < \Gamma < \frac{2}{z-\zeta}, \qquad 1 \leqslant \text{integer } \zeta \leqslant z \tag{25}$$

In Eq. (25) n denotes the initial total number of particles per unit area, and it is assumed that the system is in contact with an infinite heat reservoir which can absorb the infinite self-energy of the collapsed ion pairs. The situation is illustrated in Fig. 1 for the case $z = 4$. The extension to rational values of z is straightforward.

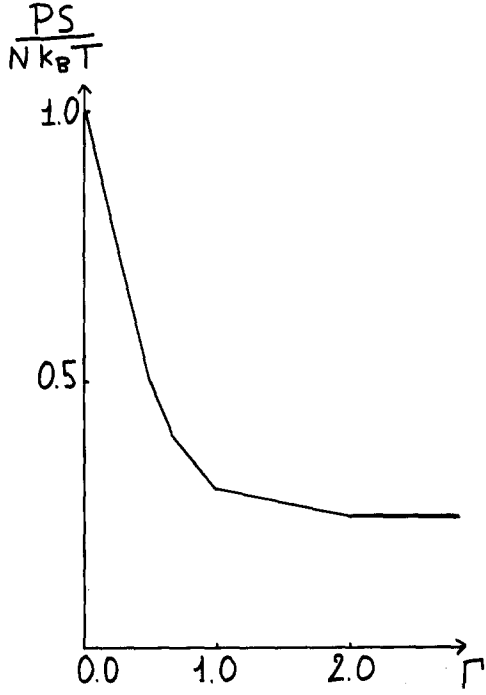

Fig. 1. Equation of state of the asymmetric two-dimensional Coulomb gas with $Z_1 = 4$, $Z_2 = -1$.

3. SHORT-RANGE PAIR CORRELATIONS

The behavior of the pair distribution functions $g_{\alpha\beta}(r)$ in classical systems is generally accepted to be dominated by the Boltzmann factor of the pair potential, $\exp[-v_{\alpha\beta}(r)/k_BT]$, in the limit $r \to 0$.[19] For the two-dimensional Coulomb gas this would imply

$$g_{\alpha\beta}(r) \underset{r\to 0}{\backsim} C_{\alpha\beta}\left(\frac{r}{L}\right)^{\Gamma Z_\alpha Z_\beta} \tag{26}$$

The divergence of the pair correlations between oppositely charged ions is in fact the salient feature, particularly near the critical coupling $\Gamma_c = 2/|Z_1 Z_2|$, where pair formation becomes dominant. The prefactors $C_{\alpha\beta}$ in Eq. (26) can be related to a free energy difference.[20] Focusing on a pair of ions labeled 1 (of species α) and 2 (of species β), we split the total potential energy of the Coulomb gas into two parts, according to

$$V_N(\mathbf{r}_1, \mathbf{r}_2, ..., \mathbf{r}_N) = v_{\alpha\beta}(r_{12}) + W_N(\mathbf{r}_1, \mathbf{r}_2, ..., \mathbf{r}_N) \tag{27}$$

where W_N is a regular function of the arguments $\mathbf{r}_1$ and $\mathbf{r}_2$ as $r_{12} = |\mathbf{r}_1 - \mathbf{r}_2| \to 0$. From the standard definition of the pair distribution functions it follows that

$$\begin{aligned} c_{\alpha\beta} &= \lim_{r_{12}\to 0} \{\exp[v_{\alpha\beta}(r_{12})/k_BT]\, g_{\alpha\beta}(r_{12})\} \\ &= \frac{S^2}{Q_N} \lim_{r_{12}\to 0} \int \cdots \int \exp[-W_N(\mathbf{r}_1, \mathbf{r}_2, ..., \mathbf{r}_N)/k_BT]\, d^2r_3 \cdots d^2r_N \\ &= \frac{S}{Q_N} \int \cdots \int \exp\{-W_N(\mathbf{r}_1, \mathbf{r}_1, \mathbf{r}_3, ..., \mathbf{r}_N)/k_BT\}\, d^2r_1\, d^2r_3 \cdots d^2r_N \end{aligned} \tag{28}$$

where use was made of translational invariance of the homogeneous plasmas. Now clearly $W_N(\mathbf{r}_1, \mathbf{r}_1, \mathbf{r}_3, ..., \mathbf{r}_N)$ is the total potential energy of a system made up of $N-2$ ions of both species located at $\mathbf{r}_3, ..., \mathbf{r}_N$, and of a single ion of charge $(Z_\alpha + Z_\beta)e$ at $\mathbf{r}_1$. The integral appearing in the last line of Eq. (28) is then precisely the configuration integral for that system, which we shall write as $Q_{N-1}(1, N-2)$ in an obvious notation. If $F^{ex}(1, N-2)$ denotes the corresponding excess Helmholtz free energy $-k_BT \ln[Q_{N-1}/S^{N-1}]$, $C_{\alpha\beta}$ takes the final form

$$\begin{aligned} C_{\alpha\beta} &= \frac{SQ_{N-1}(1, N-2)}{Q_N(0, N)} = \frac{Q_{N-1}(1, N-2)/S^{N-1}}{Q_N(0, N)/S^N} \\ &= \exp\{-[F^{ex}(1, N-2) - F^{ex}(0, N)]/k_BT\} \end{aligned} \tag{29}$$

This general result is particularly transparent in the symmetric Coulomb gas. Consider first the case of C_{12}. Since $Z_1 + Z_2 = 0$ in the symmetric case the composite particle at $\mathbf{r}_1$ has zero charge and hence does not contribute to the excess free energy, so that

$$C_{12} = \exp\{-[F^{ex}(N-2) - F^{ex}(N)]/k_B T\}$$
$$= \exp(\mu^{ex}/k_B T) \tag{30}$$

where μ^{ex} is the excess chemical potential of a pair of oppositely charged particles. This relation allows us to extract the chemical potential directly from the small r behavior of $g_{12}(r)$, a route to thermodynamics which proves to be very useful in practice (see Sections 4 and 5). Equation (30) is reminiscent of a similar result for fluids of hard-core particles (hard disks in two dimensions),[21] but it cannot be exploited in practice in the latter case since $g(r)$ is identically zero for r less than the hard-core diameter.

We next apply the general relation (29) to $g_{11}(r) = g_{22}(r)$ in the symmetric Coulomb gas ($Z_1 = -Z_2 = 1$). The composite particle at $\mathbf{r}_1$ carries now a charge $\pm 2e$, and it is immediately clear that the free energy $F^{ex}(1, N-2)$ will be finite only for $\Gamma < \Gamma_c/2 = 1$; at $\Gamma = 1$ this doubly charged ion will collapse with an appositely charge particle, and the free energy goes to $-\infty$, so that $C_{11} \equiv C_{22}$ diverges in the limit $\Gamma \to 1$. This means that the function $y_{11}(r) = \exp[v_{11}(r)/k_B T]\, g_{11}(r)$ is singular at the origin for $\Gamma > 1$, so that $g_{11}(r)$ ceases to behave as indicated by Eq. (26) in the range $1 < \Gamma < 2$.

An explicit computation of the leading power in the small r behavior of $g_{11}(r)$, i.e., the power α for which $\lim_{r \to 0} r^{-\alpha} g_{11}(r) = C$, $0 < C < \infty$, shows that it can be obtained from the behavior of $\exp[-\beta U_{11}(r)]$, where $U_{11}(r)$ is the potential of mean force between two positive ions (species 1) in the presence of a single ion of opposite charge (species 2)[38]; the result is the following:

$$g_{11}(r) \underset{r \to 0}{\sim} r^{\Gamma} \qquad \text{for} \quad \Gamma < 1 \tag{31a}$$

$$g_{11}(r) \underset{r \to 0}{\sim} r^{2-\Gamma} \qquad \text{for} \quad 1 < \Gamma < 2 \tag{31b}$$

The weaking of the short-range correlations between charges of the same sign for $\Gamma > 1$ is a manifestation of pair formation at low temperatures: the total charge of a tightly bound pair of oppositely charged particles being zero, a third ion can come very close to the homologous ion of the pair, since the electric field of the latter ion is effectively screened by its partner of opposite charge.

The extension of the result (31) to the dissymmetric case is straightforward; for integer $z = |Z_1/Z_2|$ it is found that

$$g_{22}(r) \underset{r \to 0}{\backsim} r^{\Gamma}, \qquad \Gamma < 1/z$$

$$\underset{r \to 0}{\backsim} r^{2-(2z-1)\Gamma}, \qquad 1/z < \Gamma < 2/z \tag{32a}$$

For $g_{11}(r)$ the situation is more complicated since the gradual weakening of the correlations between two "polyions" involves an increasing number of intermediate "counterions." Thus we expect z successive changes of the small r behavior of $g_{11}(r)$ in the range $1/z < \Gamma < 2/z$, of the form[39]

$$g_{11}(r) \underset{r \to 0}{\backsim} r^{\Gamma z^2}, \qquad \Gamma < 1/z$$

$$\underset{r \to 0}{\backsim} r^{2m + [z^2 - (1/2)m(4z+1-m)]\Gamma}; \qquad \frac{2}{2z-m+1} < \Gamma < \frac{2}{2z-m}$$

$$(1 \leqslant m \leqslant z) \tag{32b}$$

An interesting implication of Eq. (32a) is that $g_{22}(r)$ will actually diverge, as $r \to 0$, whenever $\Gamma > 2/(2z -)$, due to the strong clustering of negative "counterions" around a highly charfed "polyion" (polycondensation).

The short-range behavior of the direct correlation functions $c_{\alpha\beta}(r)$ can be deduced from Eqs. (31) and (32) via the OZ relations. Using the elementary properties of Hankel transforms, we find for the symmetric case ($z = 1$) in k-space

$$\hat{c}_{11}(k) \underset{k \to \infty}{\backsim} \hat{h}_{11}(k) \backsim k^{-2-\Gamma}, \qquad \Gamma < 2/3$$

$$\underset{k \to \infty}{\backsim} \hat{h}_{12}^2(k) \backsim k^{-4+2\Gamma}, \qquad 2/3 < \Gamma < 2 \tag{33a}$$

$$\hat{c}_{12}(k) \underset{k \to \infty}{\backsim} \hat{h}_{12}(k) \backsim k^{-2+\Gamma}, \qquad \Gamma < 2 \tag{33b}$$

and similarly, for the $\hat{\gamma}_{\alpha\beta} = \hat{h}_{\alpha\beta} - \hat{c}_{\alpha\beta}$:

$$\hat{\gamma}_{11}(k) \underset{k \to \infty}{\backsim} \hat{h}_{12}^2(k) \backsim k^{-4+2\Gamma}, \qquad \Gamma < 2 \tag{34a}$$

$$\hat{\gamma}_{12}(k) \underset{k \to \infty}{\backsim} \hat{h}_{11}(k)\, \hat{h}_{12}(k) \backsim k^{-4}, \qquad \Gamma < 2/3$$

$$\underset{k \to \infty}{\backsim} \hat{h}_{12}^3(k) \backsim k^{-6+3\Gamma}, \qquad 2/3 < \Gamma < 2 \tag{34b}$$

Returning to r space, we conclude that $c_{12}(r)$ exhibits the same singularity as $g_{12}(r)$ at the origin, while $c_{11}(r)$ becomes singular (behaving like $r^{2-2\Gamma}$) when $\Gamma > 1$. Similarily we find that

$$\gamma_{11}(r) = h_{11}(r) - c_{11}(r) \underset{r \to 0}{\sim} r^{2-2\Gamma} \tag{35a}$$

$$\gamma_{12}(r) = h_{12}(r) - c_{12}(r) \underset{r \to 0}{\sim} r^{2}, \qquad \Gamma < 2/3$$

$$\underset{r \to 0}{\sim} r^{4-3\Gamma}, \qquad 2/3 < \Gamma < 2 \tag{35b}$$

so that $\gamma_{11}(r)$ becomes singular when $\Gamma > 1$, while $\gamma_{12}(r)$ becomes singular when $\Gamma > 4/3$. These singularities will have important implications in the next section. Equations (33)–(35) can be casily generalized to arbitrary z.

4. APPROXIMATE THEORIES OF PAIR STRUCTURE

We now turn to the investigation of a number of approximate theories for the explicit calculation of the pair distribution functions, of the internal energy [via Eq. (20)] and of the chemical potential [via Eq. (30)] of the two-dimensional Coulomb gas. The simplest of these theories is the mean field Poisson–Boltzmann (PB) theory, which supplements the exact relation (21) by the approximation

$$g_{\alpha\beta}(r) = \exp\{-Z_\beta e \psi_\alpha(r)/k_B T\} \tag{36}$$

This amounts to replacing the potential of mean force by the product $Z_\beta e\psi_\alpha(\mathbf{r})$, and hence neglects correlations between particles in the polarization "cloud" surrounding particle α. Since the Coulomb potential is the Green's function for the Laplace operator, the PB pair distribution functions can be cast in the integral form

$$g_{\alpha\beta}(r) = \exp\left\{-\frac{1}{k_B T}\left[v_{\alpha\beta}(r) + \sum_{\gamma=1}^{2} n_\gamma h_{\alpha\gamma}(r) * v_{\gamma\beta}(r)\right]\right\} \tag{37}$$

where $*$ denotes a convolution product. Equation (37) will be useful below, but for practical calculations, the differential form of the PB equation is better suited. Combining Eqs. (21) and (36), and making the change of variables $y = \ln(r/a_1)$, $\Phi_\alpha(y) = \Psi_\alpha(r)/e$, we obtain the differential equations

$$\Phi_\alpha''(y) = 2ze^{2y}\{\exp[\Gamma\Phi_\alpha(y)] - \exp[-\Gamma z\Phi_\alpha(y)]\} \tag{38}$$

which must be solved, subject to the boundary conditions

$$\lim_{y \to +\infty} \Phi_\alpha(y) = 0 \tag{39a}$$

$$\lim_{y \to -\infty} \Phi'_\alpha(y) = -Z_\alpha, \qquad \alpha = 1, 2 \tag{39b}$$

Since $\Phi_\alpha(y) \simeq -Z_\alpha y$ as $y \to -\infty$, the r.h.s. of Eq. (38) behaves as $\exp[y(2-\Gamma z)]$ in that limit, so that the boundary condition (39) can no longer be satisfied for $\Gamma > 2/z$, which corresponds precisely to the collapse temperature (10).

The PB approximation is internally consistent only in the symmetric case ($z = 1$). For $z \neq 1$, one finds $Z_1 \Phi_2(y) \neq Z_2 \Phi_1(y)$, and hence according to Eq. (36), $g_{12}(r) \neq g_{21}(r)$. Among other defects, this inconsistency leads to two different estimates of the compressibility. According to Eqs. (24) and (13) the latter quantity can be indifferently expressed as

$$nk_B T\chi_T = x_1 \frac{S_{11}(0)}{x_1^2} + x_2 \frac{S_{12}(0)}{x_1 x_2}$$

$$= 1 + 2 \int_0^\infty [h_{11}(x) + h_{12}(x)] x \, dx \tag{40a}$$

or

$$nk_B T\chi_T = x_1 \frac{S_{21}(0)}{x_1 x_2} + x_2 \frac{S_{22}(0)}{x_2^2}$$

$$= 1 + 2z \int_0^\infty [h_{21}(x) + h_{22}(x)] x \, dx \tag{40b}$$

Both expressions can be explicitly evaluated by an integration by parts and use of Eqs. (36), (21), and (39b). The result is

$$nk_B T\chi_T = 1 + (\Gamma/4) z^2 \tag{41a}$$

$$nk_B T\chi_T = 1 + \Gamma/4 \tag{41b}$$

which should be compared to the exact result (24)

$$nk_B T\chi_T = [1 - (\Gamma/4) z]^{-1} \tag{42}$$

Only for the symmetric case ($z = 1$) do both expressions (41) agree; as expected the discrepancy with respect to the exact result (42) increases with Γ.

Numerical solutions of Eq. (38) are easily obtained by a standard Runge–Kutta method. The internal energy follows then directly from Eq. (23). PB energies for the symmetric Coulomb gas ($z=1$) are listed in Ref. 11 and in Table I, while some values for the asymmetric case $z=2$ are given in Table II. Least-squares fits to the calculated energies near $\Gamma=\Gamma_c=2/z$ show that the PB energy diverges logarithmically at the collapse temperature, so that the specific heat diverges like $(T-T_c)^{-1}$; this mean field value $\alpha=1$ of the "critical" exponent should be compared to the expected value $\alpha=2$.[6,8] Finally, in the symmetric Coulomb gas it is easily seen from Eqs. (23), (30), and (36) that the excess chemical potential of an ion pair is exactly twice the excess internal energy per ion. This estimate of μ^{ex} is clearly not consistent with the value which would be obtained by thermodynamic integration of the excess internal energy.

Linearization of Eq. (38) leads directly to the familiar Debye–Hückel result:

$$\psi_\alpha(r)=Z_\alpha e K_0(k_D r) \tag{43}$$

where K_0 denotes the zeroth-order modified Bessel function of the second kind and k_D is the Debye wave number defined in Eq. (18). Equation (23) yields directly the reduced excess internal energy per particle:

$$u^*_{DH}=\frac{\beta U^{ex}_{DH}}{N}=-\frac{k_D^2}{4\pi n}\left[\ln\left(\frac{k_D L}{2}\right)+\gamma\right] \tag{44}$$

where γ is Euler's constant; Eq. (44) should be compared to the corresponding three-dimensional result $u^*_{DH}=\beta U^{ex}_{DH}/N=-k_D^3/(8\pi n)$. Equation (44) gives the correct weak-coupling ($\Gamma=0$) limit of the energy. As can be seen from Tables I and II, u_{DH} deviates rapidly from the corresponding PB values as Γ increases; in particular u_{DH} is everywhere a continuous function of $\Gamma>0$, so that Debye–Hückel theory "misses" the collapse, as a result of the linearization.

It is well known that the DH approximation is equivalent to making the RPA assumption: $\hat{c}^s_{\alpha\beta}(k)=0$ in Eq. (19). Many improvements over the RPA have been suggested in the literature. One, which has been widely applied to Coulombic systems, is the STLS approximation.[22] For the symmetric ($z=1$) plasma this approximation leads to the following expressions for the short-range part of the direct correlation functions:

$$\hat{c}^s_{11}(k)=-\frac{k_D^2}{2\pi n k^2}\int_0^k h_{11}(k')k'\,dk' \tag{45}$$

$$\hat{c}^s_{12}(k)=\frac{k_D^2}{2\pi n k^2}\int_0^k h_{12}(k')k'\,dk' \tag{46}$$

Table I. Excess Internal Energy per Ion and Excess Chemical Potential of an Anion–Cation Pair for the Symmetric Two-Dimensional Coulomb Gas[a]

	$u = U^{ex}/Ne^2$					μ^{ex}/e^2		
Γ	DH	STLS	PB	HNC	MC	PB	HNC	MC
0.1	0.2870	0.2859	0.2862	0.2864		0.5728	0.5740	
0.5	−0.1153	−0.1464	−0.1381	−0.1344		−0.2762	−0.2511	
1.	−0.2886	−0.4610	−0.3916	−0.3791	−0.40	−0.7832	−0.7352	−0.48
1.5	−0.3900		−0.6971		−0.80	−1.3942		−0.9
1.8	−0.4356		−1.086		< -1.40	−2.172		−1.3

[a] DH, Debye–Hückel; PB, Poisson–Boltzmann; HNC, hypernetted chain; MC refers to the Monte Carlo results given in more detail in Table IV. μ^{ex} is calculated via Eq. (30). All results are given for $L = a_1$.

Table II. Excess Internal Energy of the Asymmetric Coulomb Gas ($Z_1 = 2$; $Z_2 = -1$) in the Debye–Hückel and Poisson–Boltzmann Approximations

	$u = U^{ex}/Ne^2$	
Γ	DH	PB
0.1	0.2275	0.2246
0.5	−0.5772	−0.7140
0.75	−0.7799	−1.3139
0.9	−0.8711	−2.0870
0.95	−0.8981	−2.7011

It is easily verified that these closure relations combined with the OZ relations (16) entail an unphysical singular behavior of $g_{11}(r)$ at the origin, for $\Gamma > 1$, which is induced by the corresponding (physical) singularity in $g_{12}(r) \backsim r^{-\Gamma}$. For $\Gamma < 1$ we obtained numerical solutions of the coupled STLS and OZ equations by a standard iterative procedure in k-space; some results for the energy are compared in Table I to the predictions of other theories. The STLS compressibility is easily derived by combining Eqs. (16), (17a), and (24) with the $k \to 0$ limit of Eqs. (45) and (46); the result is

$$nk_B T\chi_T = [1 - \Gamma/2]^{-1} \tag{47}$$

which is identical with the corresponding STLS results for the two-dimensional one-component plasma.[23] Note that, contrarly to the PB approximation for the symmetric Coulomb gas, STLS theory does not predict the correct small-Γ behavior of the exact compressibility (24).

Similarily one can easily check that the familiar Born–Green–Yvon integral equation leads to divergent integrals for $\Gamma > 1$. More interesting is the failure of hypernetted chain (HNC) theory, which is generally accepted as being the most accurate of the standard integral equations for Coulombic systems.[24] HNC and PB theories are in fact intimately related,[25] since the former amounts to replacing the bare Coulomb potentials $v_{\gamma\beta}(r)$ by the "renormalized" potentials $-k_B T c_{\gamma\beta}(r)$ in the convolution product appearing in the PB approximation (37), in order to account for correlations. Using the OZ relations (16) and the definition $\gamma_{\alpha\beta} = h_{\alpha\beta} - c_{\alpha\beta}$, the HNC closure reads for the symmetric Coulomb gas

$$\begin{aligned} g_{\alpha\beta}(r) &= \exp[-v_{\alpha\beta}(r)/k_B T + \gamma_{\alpha\beta}(r)] \\ &= \left(\frac{r}{L}\right)^{(-1)^{\alpha+\beta}\Gamma} \exp[\gamma_{\alpha\beta}(r)] \end{aligned} \tag{48}$$

Focusing on $g_{11}(r)$, it is clear that (48) is incompatible with the small-r behaviour described by Eqs. (31) and (35a) when $\Gamma > 1$, so that the HNC equation admits no solution for $1 < \Gamma < 2$. This can be traced back to the singular behavior of $c_{11}(r)$ in that range. It is interesting to note that the Percus–Yevick (PY) closure, which amounts to linearizing Eq. (48) with respect to $\gamma_{\alpha\beta}$, does not lead to any inconsistency for correlations between ions of the same species, but becomes inconsistent for opposite ion correlations when $\Gamma > 4/3$. But it is well known that PY theory is not applicable to Coulombic systems, because it does not lead to screening (failure at large r).

We have obtained numerical solutions of the HNC equation for the symmetric Coulomb gas, for $\Gamma < 1$, by adapting the procedure used earlier for the two-dimensional one-component plasma.[26,27] The resulting energies and chemical potentials are compared to the predictions of other theories in Table I. The compressibilities calculated from the various theories are compared to the exact result (24) in Fig. 2. In Fig. 3 we compare the HNC and PB results for the two pair distribution functions $g_{11}(r)$ and $g_{12}(r)$ at $\Gamma = 1$, to the Monte Carlo data to be discussed in the next section. While the HNC and PB pair distribution functions are in reasonable agreement, they differ significantly from the "exact" Monte Carlo results at small r; this leads in particular to a poor estimate of the chemical potential via Eq. (30).

5. MONTE CARLO STUDY OF ION PAIRING

It was shown in the preceding section that all standard approximation schemes for Coulombic systems fail when applied to the two-dimensional Coulomb gas, for couplings $\Gamma > 1$ (or $\Gamma > 1/z$ in the asymmetric case), with the exception of Poisson–Boltzmann theory, which yields solutions up to $\Gamma = 2$ (or $\Gamma = 2/z$). This failure is intimately linked to the (integrable) singularity of $g_{12}(r)$, which induces a singularity in $c_{11}(r)$ and a change in the small-r behavior of $g_{11}(r)$ for $\Gamma > 1$ and of $g_{11}(r)$ and $g_{22}(r)$ for $\Gamma > 1/z$. We have attributed the unusual behavior of the correlation functions to the increasing weight of pairing of oppositely charged ions as Γ exceeds 1; this pairing leads to complete collapse as Γ approaches the critical value $\Gamma = 2$. PB theory cannot give a correct description of this mechanism, since it ignores correlations, and hence pairing between ions in the "polarization cloud" surrounding any given ion.

In the absence of any reliable theory in the range $1 < \Gamma < 2$, we have carried out some preliminary Monte Carlo simulations to gain a qualitative understanding of ion pairing in a symmetrical Coulomb gas ($z = 1$).

Simulation of the two-dimensional Coulomb gas involves two fun-

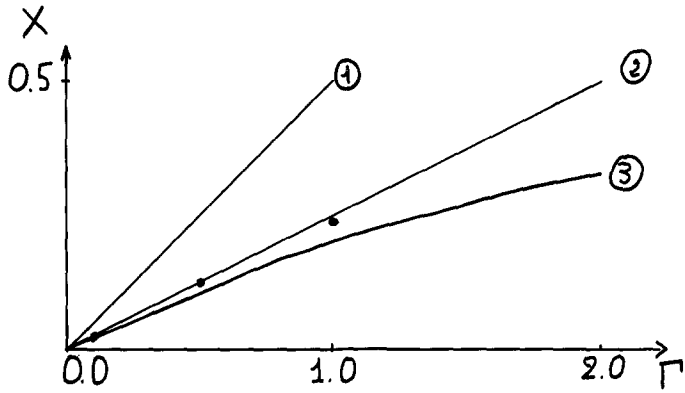

Fig. 2. Excess inverse isothermal compressibility $X = 1 - (nk_B T\chi_T)^{-}$ of the symmetric two-dimensional Coulomb gas; 1, STLS result (47); 2, exact result (42); 3, PB result (41); dots, numerical HNC results.

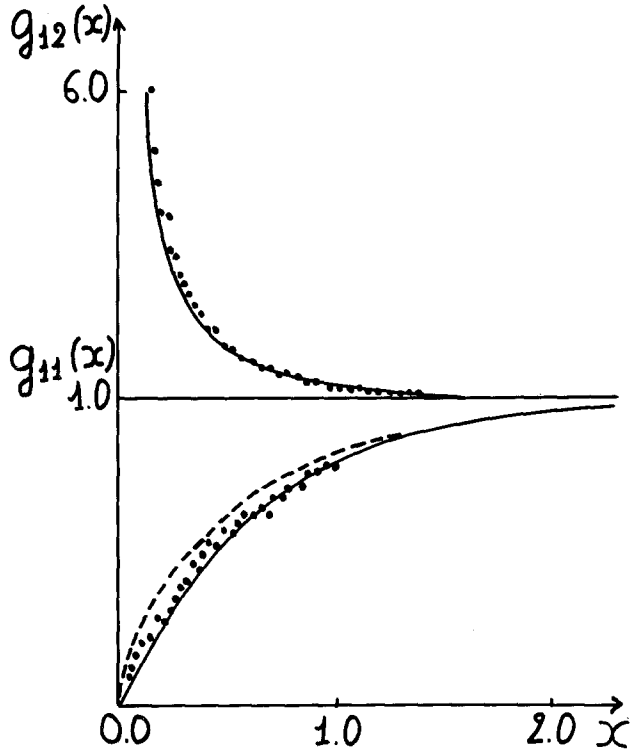

Fig. 3. Pair distribution functions $g_{11}(x)$ (lower curves) and $g_{12}(x)$ (upper curves) versus $x = r/a_1$ for the symmetric two-dimensional Coulomb gas at $\Gamma = 1$. Solid curves, Poisson–Boltzmann theory; dashed curve, HNC theory (g_{12} in this approximation is indistinguishable from the Poisson–Boltzmann result); dots, Monte Carlo results.

damental difficulties. The first of these is the well-known problem of correctly handling the infinite range of the Coulomb potential when simulating a small periodic sample. For strong couplings ($\Gamma \gg 1$), this problem is adequately solved by summing the interaction between two ions over the infinite array of their periodic images (Ewald method[28]). However, numerical evidence from Monte Carlo studies on the one-component plasma[28] and on simple electrolytes[29] in three dimensions indicates that for intermediate couplings ($\Gamma \simeq 1$), the simpler "nearest image convention" (where each ion interacts only with the nearest periodic image of all other ions) may be sufficiently accurate. We have checked the nearest image convention in two dimensions by examining the one-component plasma at $\Gamma = 2$, a case that is exactly soluble.[1] Results of three Monte Carlo runs are summarized in Table III: the number dependence of the computed energy is seen to be relatively weak, and a 5% accuracy is already achieved with $N = 100$ ions. Since we were essentially interested in ion pairing, for which short-range correlations are predominant, we have used the nearest image convention in our simulations of the two-component Coulomb gas.

The second difficulty in these simulations is precisely linked to the strong Coulomb attraction between oppositely charged ions when they are very close. Although this singularity is formally integrable up to $\Gamma = 2$, the corresponding Boltzmann factor diverges as $r \to 0$, so that a careful sampling of close ion pairs is needed in order to obtain good estimates of thermodynamic properties, like the energy. The difficulty is illustrated by the fact that near $\Gamma = 2$, the specific heat diverges as the square of the energy, which means that fluctuations in energy become very large in the canonical ensemble.

The main weakness of the standard Metropolis scheme[30] as applied to the present model is that it does not distinguish between tightly bound

Table III. Number Dependence of the Monte Carlo Estimates for the Excess Internal Energy of the Two-Dimensional One-Component Plasma (OCP) at $\Gamma = 2$, Using the Nearest Image Convention[a]

N	N_c	$u = U^{ex}/Ne^2$
64	6250	-0.1545 ± 0.01
100	3000	-0.1525 ± 0.005
196	1500	-0.1505 ± 0.003
∞	(exact)	-0.1443

[a] N is the number of particles in the sample and N_c the number of trial moves per ion generated during the runs. The exact result is from Ref. 1.

and weakly bound ion pairs; the use of a unique maximum trial displacement does not allow an efficient sampling of configuration space. This defect can be partly overcome by reformulating the canonical partition function for $N/2$ positive and $N/2$ negative ions in terms of $N/2$ pairs. Following the procedure outlined by Stillinger and Lovett,[31] all ions of opposite charges are paired in a unique way at the beginning of a Monte Carlo run. Trial configurations are generated by moving ion pairs in two steps: first, the center of mass of the pair is displaced inside a disk (or square) of radius Δ_1; next the relative position vector of the two ions in the pair is displaced inside a disk (or square) of radius Δ_2. The reformulation of the partition function in terms of ion pairs leads to configurational restrictions which can be taken care of by introducing "steric hindrance" potentials acting between two ion pairs[31]; these prevent ion exchanges between pairs and are easily incorporated into the Monte Carlo program. The advantage of this second procedure (method 2) over the more standard algorithm in which ions are moved individually (method 1) is twofold. First, by adjusting the values of Δ_1 and Δ_2, a more efficient sampling of close pair configurations can be achieved. Although we have not attempted a systematic optimization in our preliminary Monte Carlo calculations, we find, as might be expected, that the ratio Δ_2/Δ_1 should be decreases with increasing Γ in order to achieve a reasonable convergence of the Monte Carlo averages. Secondly, method 2 allows an easy and unambiguous definition of the distribution function of pair separations, $P(r)$, which is quite different from the pair distribution function $g_{12}(r)$. $P(r)\,dr$ is defined as being the man number of pairs of length falling in the range $[r, r+dr]$, divided by the total number of pairs (i.e., $N/2$). The normalization is such that

$$\int_0^\infty P(r)\,dr = 1$$

The numerical estimate of the function $P(r)$ is not practicable within method 1. It must be stressed, however, that methods 1 and 2 are equivalent in the sense that they would lead to identical expectation values in the limit of infinitely long Monte Carlo chains.

We have carried out Monte Carlo runs using both methods and two sample sizes ($N=100$ and $N=196$), for $\Gamma=1$, 1.5, and 1.8. Some of the results of these simulations are summarized in Table IV in Figs. 3–6. The runs at $\Gamma=1$ pose no particular problem: there is no significant N dependence of the results and the Monte Carlo estimates of the energy fall very close to (although slightly below) the predictions of PB and HNC theories. The difference between the chemical potentials estimated from Eq. (30) are much larger, stressing the lack of thermodynamic consistency of the

Table IV. Monte Carlo Results for the Symmetrical Two-Dimensional Coulomb Gas[a]

Γ	N	Method	N_c	$u = U^{ex}/Ne^2$	μ^{ex}/e^2	C_S^{ex}/Nk_B	f
1.0	100	1	5000	-0.398 ± 0.005			
1.0	196	2	3570	-0.400 ± 0.01	-0.48	0.8 ± 0.1	0.74
1.5	100	1	10000	-0.80 ± 0.07	-0.98	3.6 ± 0.4	
1.5	100	2	6800	-0.77 ± 0.03	-0.86	3.4 ± 0.4	
1.5	196	2	3500	-0.88 ± 0.03	-0.90		0.81
1.5	196	2	2000	-0.84 ± 0.03	-0.87		0.80
1.8	100	2	10000	-1.45 ± 0.1	-1.18	$\gtrsim 9.5$	
1.8	196	2	4500	-1.35 ± 0.1	-1.37		0.84

[a] Notation is as in Table III. μ^{ex} is the excess chemical potential of an anion–cation pair, estimated via Eq. (30). C_S^{ex} is the excess specific heat per unit area, estimated from fluctuations of the internal energy, which are very large as $\Gamma \to 2$. f is the fraction of ion pairs of length $< a_1$.

approximate theories. It must be stressed, however, that extrapolation of the Monte Carlo data $r = 0$ is delicate, because of the statistical uncertainties for small r. The distribution of pair separations $P(r)$ is a flat function of r, indicating only a relatively weak tendency towards ion pairing at twice the collapse temperature. The situation changes dramatically as Γ is increased. At $\Gamma = 1.5$, the $P(r)$ histogram in Fig. 5 exhibits a sharp maximum near the origin, followed by a slowly decreasing tail. As expec-

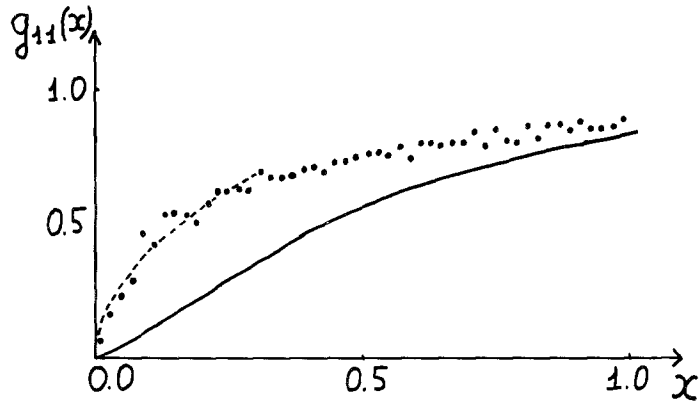

Fig. 4. $g_{11}(x)$ as a function of $x = r/a_1$ for the symmetric two-dimensional Coulomb gas at $\Gamma = 1.5$. Solid curve, Poisson–Boltzmann result; dots, Monte Carlo results; the dashed curve is a least-squares fit of the form $cx^{0.5}$ through the MC data, showing the compatibility with Eq. (31b).

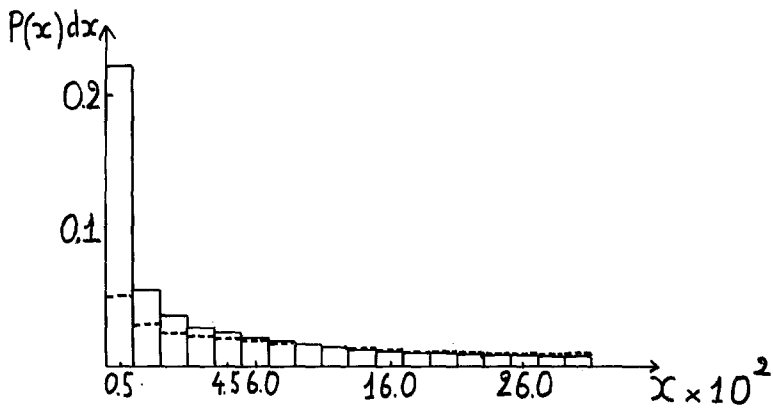

Fig. 5. Histogram of pair distances $P(x)$ as a function of $x = r/a_1$, for the symmetric two-dimensional Coulomb gas at $\Gamma = 1.5$ (dashes) and $\Gamma = 1.8$. Notice the changes of scale on the x axis.

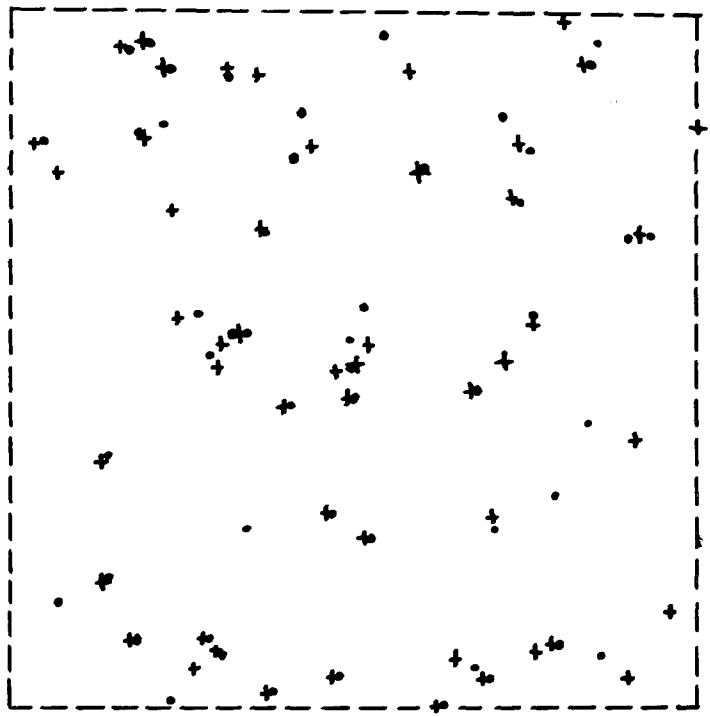

Fig. 6. A typical equilibrium configuration generated by a Monte Carlo run on the symmetric two-dimensional Coulomb gas at $\Gamma = 1.8$. +, cations; ●, anions.

ted, this tendency is considerably enhanced at $\Gamma = 1.8$. Meanwhile the fraction f of pair separated by a distance less than the characteristic interionic spacing a_1

$$f = \int_0^{a_1} P(r)\, dr \tag{49}$$

increases only moderately with Γ, indicating that even at $\Gamma = 1.8$, a sizable fraction of ions are unpaired on the average. Thus the two-dimensional Coulomb gas above $\Gamma = 1$ appears as a mixture of rather closely bound ion pairs forming dipoles of variable length, and free ions; the situation is clearly reminiscent of ion pairing in electrolyte solutions, and a crude calculation based on the classic Bjerrum model is sketched in the Appendix.

The presence of an increasing number of very close ion pairs leads to large fluctuations in the total energy which are responsible for the large statistical uncertainties on the energy estimates quoted in Table IV for $\Gamma = 1.5$ and 1.8. Although methods 1 and 2 yield compatible results, we observed that the convergence of the statistical averages with the number of configurations is rather sensitive to the values chosen for the maximum displacements, espcially Δ_2. In order to minimize the asymptotic variance of the Monte Carlo averages, a more efficient sampling algorithm, which is better adapted to the delicate ion pair equilibrium, is clearly needed. A possible alternative is the "force bias sampling," suggested by Kalos[32]; an application of this method to the two-dimensional Coulomb gas is being planned.

Although subject to caution, our Monte Carlo estimates of the internal energy lie clearly below the Poisson–Boltzmann results. The latter also fail to reproduce the characteristic small-r behavior of $g_{11}(r)$ for $\Gamma > 1$, embodied in Eq. (31); despite the large statistical scatter, the Monte Carlo data are clearly compatible with this behavior, as illustrated in Fig. 4.

The predominance of pair formation for $\Gamma > 1$ is easily visualized by examining "snapshots" of well-equilibriated configurations generated during Monte Carlo runs. Close examination of a typical example reproduced in Fig. 6 shows the existence of a high proportion of close pairs of oppositely charged ions, as well as the presence of a few triplets, which are the physical original of the "softening" of the correlations between ions of the same sign, as explained in Section 3 [see Eq. (31)]. More generally most ions are gathered in clusters, leaving large portions of the available surface blank, so that the plasma appears as highly inhomogeneous on the scale of a few interionic spacings. Among the interesting qualitative features revealed by these "snapshots" is the filamentary (as opposed to compact) topology of the clusters, which is certainly linked to the anisotropic nature

of the charge–dipole and dipole–dipole interactions, and the possible existence of a percolation threshold depending on Γ. These interesting questions clearly deserve a more detailed investigation.

6. CONCLUSIONS

Focusing on the symmetric Coulomb gas, we may summarize the main results of the present study as follows. Up to $\Gamma = 1$, corresponding to twice the collapse temperature, the model behaves essentially as a fully ionized plasma, and it pair correlations are adequately described by the standard theories of Coulombic fluids.[24] In the range $1 < \Gamma < 2$, pair correlations are strongly affected by the formation of close ion pairs and larger clusters. This mechanism is not correctly handled by the usual tools of the theory of ionic liquids[3]; in particular the nonexistence of solutions of the standard integral equations, like the HNC closure, is an obvious symptom of this failure to describe the gradual recombination of oppositely charged ions. This recombination leads to the singularity of the direct correlation function $c_{11}(r)$ and to the softening of the correlations embodied in Eq. (31), for $\Gamma > 1$.

Although the existence of a "chemical" ion-pair equilibrium leads to severe ergodicity problems in computer simulations, which are reminiscent of similar difficulties encountered in numerical studies of the three-dimensional "primitive model" of electrolytes or molten salts,[35] our preliminary Monte Carlo computations do reveal some very interesting qualitative features of the cluster formation. A quantitative understanding of the static and kinetic aspects of this purely classical "ionization" equilibrium and cluster formation requires more extensive simulations. Further work along these lines, as well as an extension to a Coulomb gas with hard cores (oppositely charged hard disks), is being planned.

ACKNOWLEDGMENTS

The authors are indebted to J. L. Lebowitz, D. Mac Gowan, and D. Nicolaides for useful comments and suggestions.

APPENDIX

In this Appendix we sketch a very simple calculations of the energy of the symmetric two-dimensional Coulomb gas which exploits the idea of a

[3] A similar conclusion has been reached for the three-dimensional "primitive model" of electrolytes (oppositely charged hard spheres) in a very instructive study of M. Gillan.[34]

"chemical" equilibrium between tightly bound ion pairs, and a plasma of fully dissociated ions. This idea goes back to Bjerrum's theory of ion pairing in the "primitive model" of electrolytes (oppositely charged hard spheres).[36] According to this idea it is assumed that a fraction α of the ions are paired into $\alpha N/2$ tightly bound pairs, while the remaining $N(1-\alpha)$ ions remain free. If the interaction between the pairs, which form neutral dipoles, and the free ions is neglected, the total partition function factors into

$$\mathcal{Q}_N = \mathcal{Q}^{\text{pair}}_{N\alpha}\, \mathcal{Q}^{\text{ion}}_{N(1-\alpha)} \tag{A.1}$$

$\mathcal{Q}^{\text{pair}}$ is evaluated by assuming that the pairs are mutually independent, and are of maximum length (anion–cation spacing) R:

$$\mathcal{Q}^{\text{pair}}_{N\alpha} = \frac{1}{(N\alpha/2)!\,(\lambda_1\lambda_2)^{N\alpha}}\, q^{N\alpha/2} \tag{A.2}$$

where

$$\begin{aligned} q &= \iint_{r_{12}<R} d^2r_1\, d^2r_2 \exp[-\Gamma \ln(r_{12}/L)] \\ &= \frac{2\pi S L^{\Gamma}}{2-\Gamma} R^{2-\Gamma} \end{aligned} \tag{A.3}$$

is the partition function of a single pair, S is the total area of the system, and λ_β is the thermal de Broglie wavelength for ion species β. The partition function for the $N(1-\alpha)$ free ions is calculated in the Debye–Hückel approximation (44). The resulting total excess free energy is given by

$$\begin{aligned} F^{\text{ex}} &= -k_B T \ln Q_N \\ &= \alpha F^{\text{ex}}_{\text{pair}} + (1-\alpha) F^{\text{ex}}_{\text{DH}} \end{aligned} \tag{A.4}$$

where Q_N is the configuration integral [cf. Eq. (5)]. The dimensionless excess free energy per ion finally reads

$$\begin{aligned} f(\alpha, \Gamma) &= \frac{F^{\text{ex}}}{Ne^2} \\ &= (1-\alpha)\ln(1-\alpha)\frac{4-\Gamma}{4\Gamma} + \frac{\alpha}{2\Gamma}\ln\alpha \\ &\quad + \frac{(1-\alpha)}{4}[\ln\Gamma + 2\gamma - 1] + \frac{\alpha}{2\Gamma}\left[1 + \ln\left(\frac{2-\Gamma}{2}\right)\right. \\ &\quad \left. - (2-\Gamma)\ln\left(\frac{R}{a_1}\right)\right] - \frac{1}{2}\ln\left(\frac{L}{a_1}\right) \end{aligned} \tag{A.5}$$

For a given Γ this free energy is minimize with respect to the "chemical" composition parameter α, leading to the equation

$$\alpha(1-\alpha)^{(\Gamma-4)/2} = \frac{2}{\Gamma^{\Gamma/2}(2-\Gamma)}\left(\frac{R}{a_1}\right)^{2-\Gamma} e^{-\gamma\Gamma} \tag{A.6}$$

For any choice of R, $\alpha \to 1$ when $\Gamma \to 2$ as expected. The precise value of R is, however, still at our disposal. Clearly R cannot be varied freely to minimize the free energy, since the latter decreases indefinitely with increasing R as a consequence of the factorization approximation (A.1), which leads to increasing double-counting of pair interactions as R increases from zero. In order to recover the correct Debye–Hückel limiting law, R must vanish when $\Gamma \to 0$. For nonzero values of Γ we have determined R/a_1 by requiring that linearization of the Poisson–Boltzmann equation be justified for all $r > R$. According to Eqs. (43) and (36) this leads to the criterion

$$\Gamma K_0(k_D R) = \Gamma K_0((4\Gamma)^{1/2} R/a_1) \simeq 1 \tag{A.7}$$

For $\Gamma \lesssim 1$, the argument of the Bessel function turns out to be quite small, so that an explicit solution of Eq. (A.7) can be obtained by replacing $K_0(x)$ by its small-x limit, $K_0(x) \simeq -\ln(x/2) + \gamma$, with the result

$$\frac{R}{a_1} = \Gamma^{-1/2} \exp(-\gamma - 1/\Gamma) \tag{A.8}$$

Since for $\Gamma > 1$, α becomes less sensitive to the precise value of R/a_1 [cf. Eq. (A.6)], we have kept the simple expression (A.8) up to $\Gamma = 2$, so that α is the solution of the equation

$$\alpha(1-\alpha)^{(\Gamma-4)/2} = 1.714 \frac{e^{-2/\Gamma}}{\Gamma(2-\Gamma)} \tag{A.9}$$

Equations (A.5), (A.8), and (A.9) determine the free energy of the Coulomb gas for each value of $\Gamma < 2$. The resulting internal energy u follows by differentiating with respect to Γ:

$$u(\Gamma) = \frac{\alpha}{2}\left[\ln\left(\frac{R}{a_1}\right) - \frac{(2-\Gamma)^2}{2\Gamma^2} - \frac{1}{2-\Gamma}\right] - \frac{(1-\alpha)}{4} \times [\ln\Gamma + 2\gamma + \ln(1-\alpha)] - \frac{1}{2}\ln\left(\frac{L}{a_1}\right) \tag{A.10}$$

This formula interpolates between the low-Γ Debye–Hückel limit and the expected $(2-\Gamma)^{-1}$ divergence due to pair collapse when $\Gamma \to 2$. Results for

Table V. Predictions of the Bjerrum Model for the Symmetrical Two-Dimensional Coulomb Gas[a]

Γ	R/a_1	α	α_{MC}	$u = U^{ex}/Ne^2$	u_{PB}	u_{MC}	μ^{ex}/e^2	μ^{ex}_{MC}/e^2
0.1	8×10^{-5}	1.8×10^{-8}		+0.287	+0.286		0.574	
0.5	0.108	0.039		−0.246	−0.138		−0.312	
1	0.207	0.174	0.21	−0.467	−0.392	−0.40	−0.776	−0.48
1.5	0.235	0.351	0.42	−0.798	−0.697	−0.80	−1.082	−0.9
1.8	0.240	0.588	0.54	−1.979	−1.086	<-1.4	−1.382	−1.3
1.9	0.241	0.746		−4.289	−1.394		−1.636	
1.95	0.241	0.857		−9.176	−1.712		−1.924	

[a] α is the fraction of ions that are bound in pairs of length $<R$ [Eq. (B.6)] and α_{MC} is the corresponding Monte Carlo estimate. u_{PB} and u_{MC} are the Poisson–Boltzmann and Monte Carlo values of the excess internal energy per ion.

the energy and the excess chemical potential per ion pair, $\mu^{ex}/e^2 = 2f - 1/2$, are compared to Poisson–Boltzmann and Monte Carlo results in Table V. The Bjerrum model is *a priori* most accurate in the two limits $\Gamma \to 0$ and $\Gamma \to 2$. In view of the simplicity of the calculation, the results can be considered as satisfactory in the intermediate coupling range as well. The model can be formalized and extended along the lines of the work of Høye and Olaussen.[37]

REFERENCES

1. B. Jancovici, *Phys. Rev. Lett.* **46**:386 (1981).
2. J. M. Kosterlitz and D. J. Thouless, *J. Phys. C* **6**:1181 (1973).
3. J. Fröhlich and T. Spencer, *Phys. Rev. Lett.* **46**:1006 (1981).
4. S. T. Chui and J. D. Weeks, *Phys. Rev. B* **14**:4978 (1976).
5. E. H. Lieb, *Rev. Mod. Phys.* **48**:553 (1976).
6. E. H. Hauge and P. C. Hemmer, *Phys. Norv.* **5**:209 (1971); see also D. Nicolaides, *Phys. Lett.* **103A**:64 (1984).
7. J. Fröhlich, *Commun. Math. Phys.* **47**:233 (1976).
8. C. Deutsch and M. Lavaud, *Phys. Rev. A* **9**:2598 (1974).
9. J. P. Hansen and I. R. McDonald, *Phys. Rev. A* **23**:2041 (1981); B. Bernu, J. P. Hansen, and R. Mazighi, *Phys. Lett.* **100A**:28 (1984).
10. See, e.g., H. Minoo, M. M. Gombert, and C. Deutsch, *Phys. Rev. A* **23**:924 (1981).
11. J. P. Hansen and P. Viot, *Phys. Lett.* **95A**:155 (1983).
12. A. Salzberg and S. Prager, *J. Chem. Phys.* **38**:2587 (1963); R. M. May, *Phys. Lett.* **25A**:282 (1967).
13. F. H. Stillinger and R. Lovett, *J. Chem. Phys.* **49**:1991 (1968).
14. D. J. Mitchell, D. A. Mc Quarrie, A. Szabo, and J. Groneveld, *J. Stat. Phys.* **17**:15 (1977).
15. Ph. A. Martin and Ch. Gruber, *J. Stat. Phys.* **31**:691 (1983).
16. L. Blum, C. Gruber, J. L. Lebowitz, and P. Martin, *Phys. Rev. Lett.* **48**:1769 (1982).

17. See, e.g., M. Parrinello and M. P. Tosi, *Riv. Nuovo Cimento* **2**(6):1 (1979).
18. G. S. Manning, *J. Chem. Phys.* **51**:925 (1969).
19. B. Widom, *J. Chem. Phys.* **39**:2808 (1963).
20. B. Jancovici, *J. Stat. Phys.* **17**:357 (1977).
21. W. G. Hoover and J. C. Poirier, *J. Chem. Phys.* **37**:1041 (1962).
22. K. S. Singwi, M. P. Tosi, R. H. Land, and A. Sjölander, *Phys. Rev.* **176**:589 (1968).
23. R. Calinon, K. I. Golden, G. Kalman, and D. Merlini, *Phys. Rev. A* **20**:329, 336 (1979).
24. M. Baus and J. P. Hansen, *Phys. Rep.* **59**:1 (1980).
25. D. Henderson and L. Blum, *J. Chem. Phys.* **70**:3149 (1979).
26. J. M. Caillol, D. Levesque, and J. J. Weiss, *Mol. Phys.* **44**:733 (1981).
27. J. P. Hansen and D. Levesque, *J. Phys. C* **14**:L603 (1981).
28. S. G. Brush, H. L. Sahlin, and E. Teller, *J. Chem. Phys.* **45**:2102 (1966).
29. J. P. Valleau and S. G. Whittington, in *Statistical Mechanics*, part A, B. J. Berne, ed. (Plenum, New York, 1977).
30. N. Metropolis, A. W. Rosenbluth, M. N. Rosenbluth, A. N. Teller, and E. Teller, *J. Chem. Phys.* **21**:1087 (1953).
31. F. H. Stillinger and R. Lovett, *J. Chem. Phys.* **48**:3858 (1968).
32. D. Cperley, G. V. Chester, and M. H. Kalos, *Phys. Rev. B* **16**:3081 (1977).
33. C. Pangali, M. Rao, and B. J. Berne, *Chem. Phys. Lett.* **55**:413 (1978).
34. M. Gillan, AERE Harwell report No. TP. 913 (1981).
35. B. Hafskjold and G. Stell, in *Statistical Mechanics*, E. Montroll and J. L. Lebowitz, eds. (North-Holland, Amsterdam, 1982).
36. N. Bjerrum, *K. Dan. Vidensk. Selsk.* **7**:9 (1926).
37. J. S. Høye and K. Olaussen, *Physica* **104A**:447 (1980); and **107A**:241 (1981).
38. P. Viot, Thèse de 3e Cycle, Université P. et M. Curie, Paris (1984).
39. J. L. Lebowitz and D. Mac Gowan, private communication.